6th International INQUA Meeting on Paleoseismology, Active Tectonics and Archaeoseismology,
19-24 April 2015, Pescina, Fucino Basin, Italy

INQUA Focus Group on Paleoseismology and Active Tectonics

paleoseismicity.org

Assessing seismic efficiency from scalar Moment-rates: an application to Mt. Etna volcano (Italy)

Azzaro, R., Barberi, G., Cannavò, F., Cocina, O., Palano, M., Scarfì, L.

Istituto Nazionale di Geofisica e Vulcanologia, OE - Sezione di Catania, Catania, Italy. Email: raffaele.azzaro@ingv.it

Abstract: *Here we propose an improved estimation of the scalar seismic (from instrumental and historical catalogues), geodetic and geologic moment-rates for the eastern flank of Mt. Etna. The estimated moment-rates have been compared in terms of seismic efficiency. Results show that all the calculated efficiency values are lower than 40%, i.e., the geodetic moment-rate estimations are generally larger than the seismic and the geologic ones. Although a number of reasons may account for the observed discrepancy, we are confident that a large amount of the deformation affecting the eastern flank occurs aseismically.*

Key words*: Mt. Etna, moment-rates, seismic efficiency, creeping faults.*

Introduction

The comparison of seismic, geologic and geodetic moment-rates can provide crucial insights for understanding fault behaviour in tectonically active zone, with obvious implications on seismic hazard assessment (Masson et al., 2005; Pancha et al., 2006; Puskas et al., 2011; Talebian, 2012). It is well acknowledged that when the seismic moment-rate is lower than geodetic or geologic ones, the exceeding moment-rate is released in aseismic mode. In fact, the observed geological and geodetic moment-rates include both elastic and inelastic deformations, and since only the elastic component is responsible for earthquakes, the comparison of these moment-rates with the seismic one do not balance in regions affected by creeping faults or where significant amounts of deformation take place plastically (Palano et al., 2011).

It is the case of Etna, where slow aseismic slip due to fault creep is a common mode of displacement along many of the fault segments in the eastern flank (Rasà et al., 1996).

A first application of the methodology to estimate and compare the scalar seismic, geodetic and geological moment-rates was recently applied at Mt. Etna (Barberi et al., 2014) following the methodology proposed for the Southern Apennines by Palano et al. (2011) and Ferranti et al. (2014). The preliminary results have been now improved by a more precise constraints on geometric and kinematic fault parameters to reduce uncertainties on the geological moment-rate estimation. The present analysis has allowed to estimate the seismic efficiency of the faults in the eastern flank of Etna, that appears essentially low due to the relevant component of the aseismic deformation.

Seismological data

In order to define the seismotectonic features of the faults in the eastern flank of Etna, we considered both long- and short-term seismicity data.

As regards the first ones, we used the huge historical data set represented by the macroseismic catalogue of earthquakes occurring at Etna from 1832 to 2013 [CMTE Working Group, 2014]. For the analysis we selected major events located in the eastern flank, i.e. 167 shocks with epicentral intensity $I_0 \geq$ V EMS (above the damage threshold) corresponding to an equivalent magnitude $M_L \geq 3.0$ according to Azzaro et al. (2011). The above thresholds represent a portion of the catalogue statistically complete, so these earthquakes may be considered as representative of the seismic cycle in the long-term (Azzaro et al., 2012b).

Regarding the short-term, the instrumental data set covers the time interval from the 2005 to 2013. The choice of this time-span is justified by the development of a modern seismic network, equipped with digital stations and broad-band sensors, allowing the detection of small magnitude events and hence the application of advanced techniques for locating epicenters.

From the initial dataset - about 4,570 seismic events with a magnitude M_L between 1.0 and 4.8 (magnitude of completeness $M_c \geq 1.5$) - we selected about 1,600 earthquakes located in the study areas of Timpe and Pernicana faults (Fig. 1). In order to better define seismic clusters or epicentre alignments, the selected earthquakes have been relocated using the tomoDDPS algorithm (Zhang et al., 2009) and the 3D velocity model of Alparone et al. (2012). Results show that seismic events tend to cluster around active faults mainly in the depth range 3-10 km in the Timpe zone, and between -1 and 3 km along the Pernicana fault.

Geodetic data

Available GPS observations collected by the Mt. Etna permanent GPS Network, spanning the 2005.00-2013.99 time interval and covering the eastern flank of Mt. Etna (Fig. 1), have been processed using the GAMIT/GLOBK software following the method described in Gonzalez and Palano (2014). Estimated geodetic velocities were referred to the "Etn@ref" reference frame (a local reference frame computed to isolate the Mt. Etna volcanic deformation from the background regional tectonic pattern; see Palano et al. 2010 for details).

The resulting velocity field confirms the seaward motion of the eastern flank of Mt. Etna. In detail, sites close to the central sector of the unstable flank are characterized by velocities up to 35 mm/yr, while moving southward or northward the velocity field decreases to values of ca. 1-2 mm/yr.

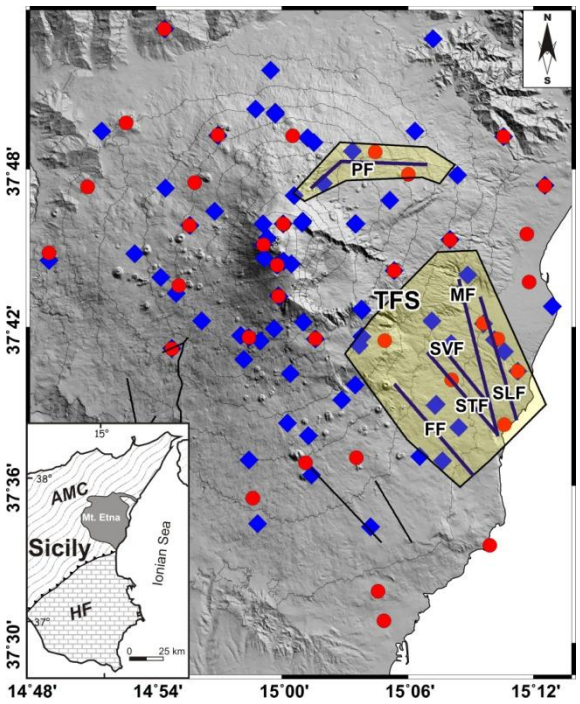

Figure 1. Sketch map of Mt. Etna. Continuous GPS stations are reported as red points, while seismic stations are reported as blue diamonds. The highlighted boxes represents the surface projection of the prismatic bodies used for the moment-rates estimations. Abbreviations: PF, Pernicana fault; FF, Fiandaca fault; SLF-MF, S. Leonardello–Moscarello fault system; STF-SVF, S. Tecla–S. Venerina fault system; TFS, Timpe fault system. The inset reports a simplified structural map of eastern Sicily; AMC: Apenninic-Maghrebian Chain; HF: Hyblean Foreland.

Geologic data

The region of Mt. Etna is characterised by intense geodynamics at the scale of the volcano, with a continuous ESE seaward sliding instability process affecting the eastern flank, which represents the result of interaction among regional stress regime, magma intrusion and basement geometry (Azzaro et al., 2013). Evidence of active tectonics is mostly distributed over the unstable sector, with a number of faults forming two main structural systems: the Timpe faults, and the Pernicana fault. The Timpe fault system crosses the central part of the eastern flank with a 20 km long and 5 km wide belt of mainly extensional structures, striking from N to NW and consisting of well-developed morphological scarps and hidden fault segments (Azzaro et al., 2012a). Their intense activity is expressed not only by seismicity but also fault creep, with geological slip-rates varying from 1.0 to 5.3 mm/yr (see Azzaro et al., 2012a for an overview). The analysis of ground deformation decennial time series (GPS, SAR) has shown that inside the Timpe system there are kinematic domains characterised by different velocity and displacements, but all showing discontinuous dynamics (Palano et al., 2008; Bonforte et al., 2011). Basically, the fairly constant mid-term (decennial) ESE seaward sliding is interrupted by sudden short-term (months to year) accelerations related to flank eruptions. Conversely, there is a general agreement on identifying the Pernicana fault system to represent the northern boundary of the unstable sector (Fig. 1). Dynamics of this important tectonic element became evident through geodetic data collected since 1997 (Azzaro et al., 2001, Palano et al., 2006), which evidenced a fairly stable slip with an average rate of about 28 mm/yr, related to the continuous long-term sliding motion of the eastern flank of the volcano toward the sea. Abrupt, even transient, increase in the seismic and geodetic strain release of the Pernicana fault has been measured during some recent flank eruptions (e.g. 2001 and 2002-03) and interpreted as a result of additional stressed induced by the magma ascent in the feeding system (Palano et al., 2008; Alparone et al., 2013; Bonaccorso et al., 2013).

In order to estimate the geologic moment-rates, we collected geometric and kinematic parameters from published and unpublished studies (see Azzaro et al., 2013 and references therein). More in detail, for each structure we considered the following parameters: length (L), strike (θ), dip (ϕ), down-dip width (H), and slip-rate (if available, we used both short- and long-term estimations). On the whole, the faults have length typically in the ~5-8 km range and down-dip width in the 1.6-4.5 km range. Slip-rates (long-term) range from 1 up to 5.2 mm/yr in the Timpe system while along the Pernicana fault the slip-rate obtained for the last millennium is much more higher, up to 24 mm/yr (Ferreli et al., 2002).

Computation of moment-rates

As a first step, taking into account the spatial distribution of the active faults and their seismogenic thickness Hs, we divided the investigated volume into prismatic bodies (Fig. 1). Then, by adopting relevant formulations (see Barberi et al., 2014 for details), we calculated for each prismatic body the scalar moment-rates.

The seismic moment-rate was calculated according to the Kostrov (1984) general formulation which takes into account the number of events occurred in the selected volume during the considered time interval. By considering both instrumental and historical earthquake catalogues, we performed two different computations. All magnitudes were converted into scalar moments through the relationship proposed for this area by Giampiccolo et al. (2007). The obtained seismic moment rates range in the interval $3.55 \cdot 10^{13}$ - $8.06 \cdot 10^{14}$ Nm/yr, and 2.2710^{14} - $1.96 \cdot 10^{15}$ Nm/yr, for the instrumental and historical catalogues, respectively.

The geodetic moment-rate was estimated by adopting the formulation proposed by Savage and Simpson (1997), which takes into account the average strain-rate tensor for the selected area, the volume of each prismatic body

and the shear modulus of rocks. The estimated geodetic moment-rate ranges in the interval $8.16 \cdot 10^{14}$ - $2.57 \cdot 10^{16}$ Nm/yr.

Lastly, the geological moment-rate was computed by using the Brune (1968) formulation which takes into account the shear modulus of the rocks involved in faulting, the dimensions (length and down-dip width) of the dislocation and the average geologic slip-rate. The calculated geological moment-rate ranges in the interval $2.16 \cdot 10^{14}$ - $3.81 \cdot 10^{15}$ Nm/yr. Figure 2 shows the values of the different typologies of moment-rates for the analysed faults.

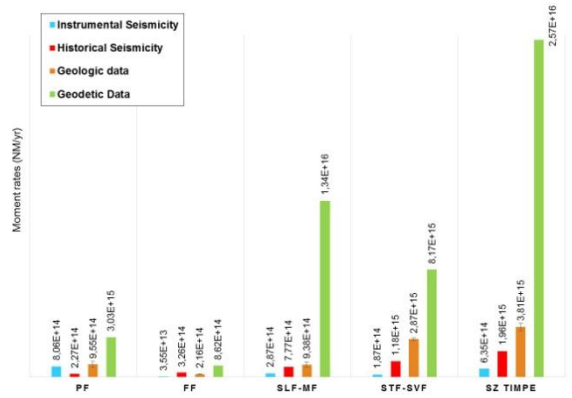

Figure 2. Seismological, geological and geodetic moment-rates obtained for the analysed structures. Abbreviations as in Fig. 1.

Results and conclusions

The comparison of moment-rates has been performed through the concept of seismic efficiency (value expressed in percentage of the seismological and geological moment-rates with respect to the geodetic one) as described in Caporali et al. (2003). The theoretical range of seismic efficiency is between 0% and 100%: the more the value close to 100%, the larger part of the deformation is released by brittle deformation, i.e. through earthquakes. Conversely, a low ratio shows an apparent seismic-moment deficit, which could indicate either a high creep component (aseismic deformation) or accumulating strain not released by seismicity. The values of seismic efficiency for the analysed fault systems are reported in Figure 3.

This result shows that, for the investigated zones, seismic efficiency values are lower than 40%, since the geodetic moment-rate estimations are generally larger than the seismic and the geologic ones. Similar results have been observed in other tectonically active areas such as the Southern Apennines in Italy (Palano et al., 2011) and the Bitlis-Zagros collisional belt in Iran (Masson et al., 2005).

In general, a number of reasons may account for the observed discrepancy among the estimated moment-rates, such as: i) uncertainties on geodetic strain rates estimations related to the station coverage, ii) uncertainties of the geologic slip-rate estimations; iii) not well constrained geometry of modelled faults, especially for down-dip width; iv) role of buried/hidden fault segments in accommodating deformation (slip-rate partitioning); v) limited length of the instrumental earthquake catalogue. Nevertheless, such a relevant difference confirms that a large amount of the deformation at Etna occurs aseismically along faults in the eastern flank, as previously suggested by field observations (Rasà et al., 1996). Although such a kind of approach is not common in volcanic areas, a relevant component of aseismic deformation has been recognised along the East African Rift System (Depréz et al., 2013), and seems to be related with the local rheological properties of the crust.

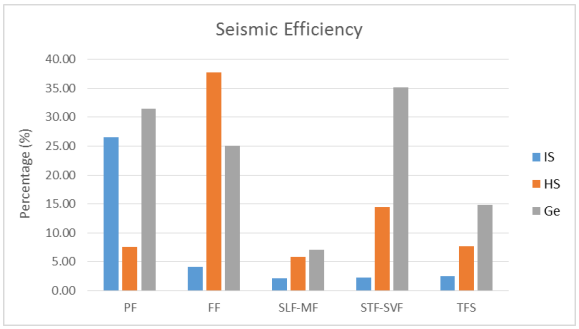

Figure 3. Values of seismic efficiency estimated for the analysed faults. Bars represent the seismological moment-rates (IS, from instrumental data; HS, from historical data) and the geological ones (Ge) expressed in terms of percentage with respect to the geodetic moment-rate.

In conclusion this study provides, for the first time, an analytical estimation of creep processes at Mt. Etna volcano by means of the deficit of seismic moment-rate calculated with respect the geodetic one. This may be viewed as a proxy of loading processes on locked fault segments prone to seismic failure, to be used with other approaches (Azzaro et al., 2013; Cannavò et al. 2014) to forecast next earthquake ruptures.

Acknowledgements: This study has benefited from funding provided by the Italian Presidenza del Consiglio dei Ministri – Dipartimento della Protezione Civile (DPC), in the frame of the 2012-14 Agreement with Istituto Nazionale di Geofisica e Vulcanologia-INGV, Project V3 "Multi-disciplinary analysis of the relationships between tectonic structures and volcanic activity". This paper does not necessarily represent DPC official opinion and policies. The authors are grateful to S. D'Amico for having provided supplementary elaborations useful for the study.

References

Alparone, S., G. Barberi, O. Cocina, E. Giampiccolo, C. Musumeci & D. Patanè, (2012). Intrusive mechanism of the 2008–2009 Mt. Etna eruption: constraints by tomographic images and stress tensor analysis. *Journal of Volcanology and Geothermal Research.* 229-230, 50-63, doi: 10.1016/j.jvolgeores.2012.04.001.

Azzaro, R., S. D'Amico & T. Tuvè, (2011). Estimating the magnitude of historical earthquakes from macroseismic intensity data: new relationships for the volcanic region of Mount Etna (Italy). *Seism. Res. Lett.* 82, 4, 533-544.

Azzaro, R., S. Branca, K. Gwinner & M. Coltelli, (2012a). The volcano-tectonic map of Etna volcano, 1:100.000 scale: an integrated approach based on a morphotectonic analysis from high-resolution DEM constrained by geologic, active faulting and seismotectonic data. *Italian Journal of Geosciences*. 131, 153-170, doi:10.3301/IJG.2011.29.

INQUA Focus Group on Paleoseismology and Active Tectonics

paleoseismicity.org

Azzaro, R., S. D'Amico, L. Peruzza & T. Tuvè, (2012b). Earthquakes and faults at Mt. Etna (southern Italy): problems and perspectives for a time-dependent probabilistic seismic hazard assessment in a volcanic region. *Bollettino di Geofisica Teorica ed Applicata*. 53, 75-88.

Azzaro, R., A. Bonforte, S. Branca & F. Guglielmino, (2013). Geometry and kinematics of the fault systems controlling the unstable flank of Etna volcano (Sicily). *Journal of Volcanology and Geothermal Research*. 251, 5-15, doi: 10.1016/j.jvolgeores.2012.10.001.

Azzaro, R., M. Mattia & G. Puglisi, (2001). Fault creep and kinematics of the eastern segment of the Pernicana Fault (Mt. Etna, Italy) derived from geodetic observation and their tectonic significance. *Tectonophysics*. 333, 401-415, doi:10.1016/S0040-1951(01)00021-X.

Barberi, G., F. Cannavò, O. Cocina, M. Palano, L. Scarfì & R. Azzaro, (2014). Comparing seismic, geodetic and geologic scalar moment-rates at Mt. Etna volcano (Italy): some preliminary results for seismogenic zones in the eastern flank. Proc. XXXIII° Convegno Nazionale GNGTS, 25-27 November 2014, Bologna (Italy), p. 32-37.

Boehm, J., B. Werl & H. Schuh, (2006). Troposphere mapping functions for GPS and very long baseline interferometry from European Centre for Medium-Range Weather Forecasts operational analysis data. *Journal of Geophysical Research*. 111, B02406, doi:10.1029/2005JB003629.

Bonaccorso, A., G. Currenti & C. Del Negro, (2013). Interaction of volcano-tectonic fault with magma storage, intrusion and flank instability: a thirty years study at Mt. Etna volcano. *Journal of Volcanology and Geothermal Researches*. 251, 127-136.

Bonforte, A., F. Guglielmino, M. Coltelli, A. Ferretti & G. Puglisi, (2011). Structural assessment of Mount Etna volcano from Permanent Scatterers analysis. *Geochemistry Geophysics Geosystems*. 12, Q02002, doi: 10.1029/2010GC003213.

Brune, J.N., (1968). Seismic moment, seismicity and rate of slip along major fault zones. *Journal of Geophysical Research*. 73 (2), 777-784, doi:10.1029/JB073i002p00777.

Cannavò, F., A. Arena & C. Monaco, (2014). Local geodetic and seismic energy balance for shallow earthquake prediction. *Journal of Seismology*. 19 (1), doi: 10.1007/s10950-014-9446-z

CMTE Working Group, (2014). *Catalogo Macrosismico dei Terremoti Etnei, 1832-2013*. INGV, Catania, http://www.ct.ingv.it/macro/etna/html_index.php.

Depréz, A., C. Doubre, F. Masson & P. Ulrich, (2013). Seismic and aseismic deformation along the East African Rift System from a reanalysis of the GPS velocity field of Africa. *Geophys. J. Int*. 193 (3), 1353-1369, doi:*10.1093/gji/ggt085*.

Ferranti, L., M. Palano, F. Cannavò, M.E. Mazzella, J.S. Oldow, E. Gueguen, M. Mattia & C. Monaco, (2014). Rates of geodetic deformation across active faults in southern Italy. *Tectonophysics*. 621, 101-122, doi:10.1016/j.tecto.2014.02.007.

Ferreli, L., A.M. Michetti, L. Serva & E. Vittori, (2002). Stratigraphic evidence of coseismic faulting and aseismic fault creep from exploratory trenches at Mt. Etna volcano (Sicily, Italy). In: *Ancient Seismites* (Ettensohn, F.R., Rast, N., Brett, C.E. eds.), Geological Society of America, Special Paper, 359, 49–62.

Giampiccolo, E., S. D'Amico, D. Patanè & S. Gresta, (2007). Attenuation and source parameters of shallow microearthquakes at Mt. Etna volcano (Italy). *Bulletin of the Seismological Society of America*. 97 (1b), 184-197, doi:10.1785/0120050252.

González, P.J. & M. Palano, (2014). Mt. Etna 2001 eruption: new insights into the magmatic system feeding and the mechanical response of the western flank from geodetic data. *Journal of Volcanology and Geothermal Research*. 274, 108-121, doi:10.1016/j.jvolgeores.2014.02.001.

Gruppo Analisi Dati Sismici, (2014). *Catalogo dei terremoti della Sicilia Orientale – Calabria Meridionale (1999–2013)*. INGV-Catania (http://www.ct.ingv.it/ufs/analisti/catalogolist.php).

Herring, T.A., (2003). MATLAB Tools for viewing GPS velocities and time series. *GPS Solutions*. 7 (3), 194-199, doi:10.1007/s10291-003-0068-0.

Kostrov, B., (1974). *Seismic moment and energy of earthquakes and seismic flow of rock*. Izv. Acad. Sci. USSR, Phys. Solid Earth, 1, 23-40.

Masson, F., J. Chéry, D. Hatzfeld, J. Martinod, P. Vernant, F. Tavakoli & M. Ghafory-Ashtiani, (2005). Seismic versus aseismic deformation in Iran inferred from earthquakes and geodetic data. *Geophys. J. Int*. 160, 217-226, doi: 10.1111/j.1365-246X.2004.02465.x.

Palano, M., M. Aloisi, M. Amore, A. Bonforte, F. Calvagna, M. Cantarero, O. Consoli, S. Consoli, F. Guglielmino, M. Mattia, B. Puglisi & G. Puglisi, (2006). Kinematic and strain analyses of the eastern segment of the Pernicana fault (Mt. Etna, Italy) derived from geodetic techniques (1997–2005). *Annals of Geophysics*. 49 (4/5), 1105-1117, doi: 10.4401/ag-3103.

Palano, M., G. Puglisi & S. Gresta, (2008). Ground deformation patterns at Mt. Etna from 1993 to 2000 from joint use of InSAR and GPS techniques. *Journal of Volcanology and Geothermal Research*. 169, 99-120, doi:10.1016/j.jvolgeores.2007.08.014.

Palano, M., M. Rossi, C. Cannavò, V. Bruno, M. Aloisi, D. Pellegrino, M. Pulvirenti, G. Siligato & M. Mattia, (2010). Etn@ref, a geodetic reference frame for Mt. Etna GPS networks. *Annals of Geophysics*. 53 (4), 48-79, doi:10.4401/af-4879.

Palano, M., F. Cannavò, L. Ferranti, M. Mattia & E. Mazzella, (2011). Strain and stress fields in the Southern Apennines (Italy) constrained by geodetic, seismological and borehole data. *Geophys. J. Int.* 187 (3), 1270–1282.

Pancha, A., J.G. Anderson & C. Kreemer, (2006). Comparison of Seismic and Geodetic Scalar Moment Rates across the Basin and Range Province. *Bulletin of the Seismological Society of America*. 96, 11-32, doi: 10.1785/0120040166.

Puskas, C., R.B. Smith, W. Chang, A.Cannaday & C.B. DuRoss, (2011). Comparison of Moment Rates from GPS observations and Late Quaternary paleoearthquakes on the Wasatch Fault, Utah. *AGU, Fall Meeting 2011*, abstract #G11A-0860.

Rasà, R., R. Azzaro & O. Leonardi, (1996). Aseismic creep on faults and flank instability at Mt. Etna volcano. In: *Volcano instability on the Earth and other planets* (McGuire, W.J., Jones, A.P., Neuberg, J. eds). Geological Society, London, Special Publications, 110, 179-192, doi: 10.1144/GSL.SP.1996.110.01.14.

Saastamoinen, J., (1972). Contribution to the theory of atmospheric refraction. *Bulletin Géodésique*. 105 (1), 279-298, doi:10.1007/BF02521844.

Savage, J.C. & R.W. Simpson, (1997). Surface strain accumulation and the seismic moment tensor. *Bulletin of the Seismological Society of America*. 87, 1345-1353.

Scarfì, L., H. Langer & A. Scaltrito, (2009). Seismicity, seismotectonics and crustal velocity structure of the Messina Strait (Italy). *Phys. Earth Planet. Inter.* 177, 65–78. http://dx.doi.org/10.1016/j.pepi.2009.07.010.

Talebian, M., (2012). Comparison of seismic, geodetic and geologic moment rates in Eastern Alborz and Kopeh Dagh. *Geosciences*. 22 (86), 183-192.

Zhang H., C. Thurber & P. Bedrosian, (2009). Joint inversion for Vp, Vs, and Vp/Vs at SAFOD, Parkfield, California. *Geochemistry Geophysics Geosystems*. 10, Q110032, doi:10.1029/2009GC002709.

INQUA Focus Group on Paleoseismology and Active Tectonics

paleoseismicity.org